

中扬子区巴东组凝灰岩层的锆石 U-Pb 年龄约束

马千里^{1,2)}, 柴嵘^{1,2)}, 杜远生^{1,2)}, 杨江海^{1,2)}, 戴贤铎^{1,2)}

1) 生物地质与环境地质国家重点实验室, 中国地质大学, 武汉, 430074;

2) 中国地质大学(武汉)地球科学学院, 武汉, 430074

内容提要:印支运动深刻地改变了华南大陆和东亚的古地理格局, 导致了大规模的海陆变迁。在扬子北缘发育有以紫红色碎屑岩为主的巴东组及相关地层, 代表了从碳酸盐岩为主的海相沉积到碎屑岩为主的陆相沉积的转变。巴东组可划分为三段, 即一、三段的紫红色粉砂岩、泥岩夹二段灰岩泥灰岩。由于巴东组三段的化石稀少, 其年代归属一直存有争议。本文运用 LA-ICP-MS 定年方法, 对新发现于鄂西秭归地区巴东组二段的凝灰岩夹层进行了锆石 U-Pb 定年。结果表明, 来自于巴东组二段中部和顶部的两件凝灰岩样品分别形成于 241.7 ± 1.7 Ma 和 237.5 ± 2 Ma。结合凝灰岩层的就位年龄和生物化石记录, 巴东组地层时代被限定为中三叠世安尼期至晚三叠世卡尼期。凝灰岩中锆石颗粒多呈长柱状, 无磨圆, 发育明显的振荡环带, 且具有与造山型岩浆锆石一致的微量元素化学特征。以巴东组灰岩为代表的“最高海相层”穿时地分布于鄂东南至川西一线, 反映了上、中扬子区由中三叠世安尼期晚期至晚三叠世卡尼期海水大规模向西退去的海陆变迁特征。

关键词:凝灰岩; 巴东组; 中扬子; 印支运动; 海陆变迁

伴随着华南、华北两大板块的汇聚碰撞(Zhang Guowei et al., 1996, 2003; Dong Yunpeng et al., 2011, 2016; Liu et al., 2015)和江南古陆的隆起(刘宝珺等, 1994; Wang Yuejun et al., 2013), 扬子板块于中一晚三叠世结束了逾 5 亿年的海相沉积, 进入三角洲-河流-湖泊的陆相沉积阶段。分布于鄂西、川东、黔北和湘西北等地的一套紫红色碎屑岩夹海相灰岩的地层——巴东组, 反映了中扬子区对于印支运动的沉积响应(Li Xubing et al., 2008; Zhao Xiaoming et al., 2010), 记录了从海到陆的重大古地理变革(Liu Zhili et al., 2001; Mei Mingxiang, 2014; Bo Jingfang et al., 2019)。然而学术界对巴东组的地层时代还缺少一致的认识, 一些学者认为巴东组为中三叠世安尼期(Yang Zunyi et al., 1982; 杨遵仪等, 2000)或是安尼期至拉丁期(赵金科等, 1962; 张振来等, 1987; 湖北省地质矿产局, 1996)沉积建造, 而其他学者则认为巴东组

有可能延续到晚三叠世(Xu Deyou, 1938; Meng Fansong et al., 2003)。

火山凝灰岩具有等时性和广布性的特点。随着近年来锆石 U-Pb 同位素测试技术的发展, 地层中凝灰岩的就位年龄逐渐成为层位对比和约束地层年代的有力工具(Macdonald, et al., 2010; Huang Hu et al., 2012)。本文报道了新发现于湖北省宜昌市秭归县两河口镇巴东组二段灰岩的凝灰岩夹层, 并对其中的岩浆锆石进行 LA-ICP-MS 分析, 综合分析结果和生物化石记录对巴东组的地层年龄进行约束, 并在此基础上进一步探究凝灰岩层与巴东组的地质意义。

1 地质背景

1.1 巴东组的地层划分与对比

德国学者 Richthofen 于 1912 年在巴东县长江沿岸建立了“巴东层”(Patung-Schichten), 原始定义

注: 本文为国家自然科学基金项目(编号 41672106)资助的成果。

收稿日期: 2019-05-03; 改回日期: 2019-07-22; 网络发表日期: 2019-08-05; 责任编委: 任东; 责任编辑: 周健。

作者简介: 马千里, 男, 1993 年生。在读博士生, 致力于造山带沉积学与盆山相互作用等领域的研究。Email: maqlcug@126.com。通讯作者: 杨江海, 男, 1984 年生。副教授, 博士生导师, 从事沉积大地构造(沉积盆地与造山带演化)、沉积物源区分析、大陆风化与气候变化等多个方向的研究。Email: yjhcg@126.com。

引用本文: 马千里, 柴嵘, 杜远生, 杨江海, 戴贤铎. 2019. 中扬子区巴东组凝灰岩层的锆石 U-Pb 年龄约束. 地质学报, 93(11): 2785~2796, doi: 10.19762/j.cnki.dizhixuebao.2019195.
Ma Qianli, Chai Rong, Du Yuansheng, Yang Jianghai, Dai Xianduo. 2019. Geochronological constraints on tuffs of the Badong Formation along the north margin of the Middle Yangtze region. Acta Geologica Sinica, 93(11): 2785~2796.

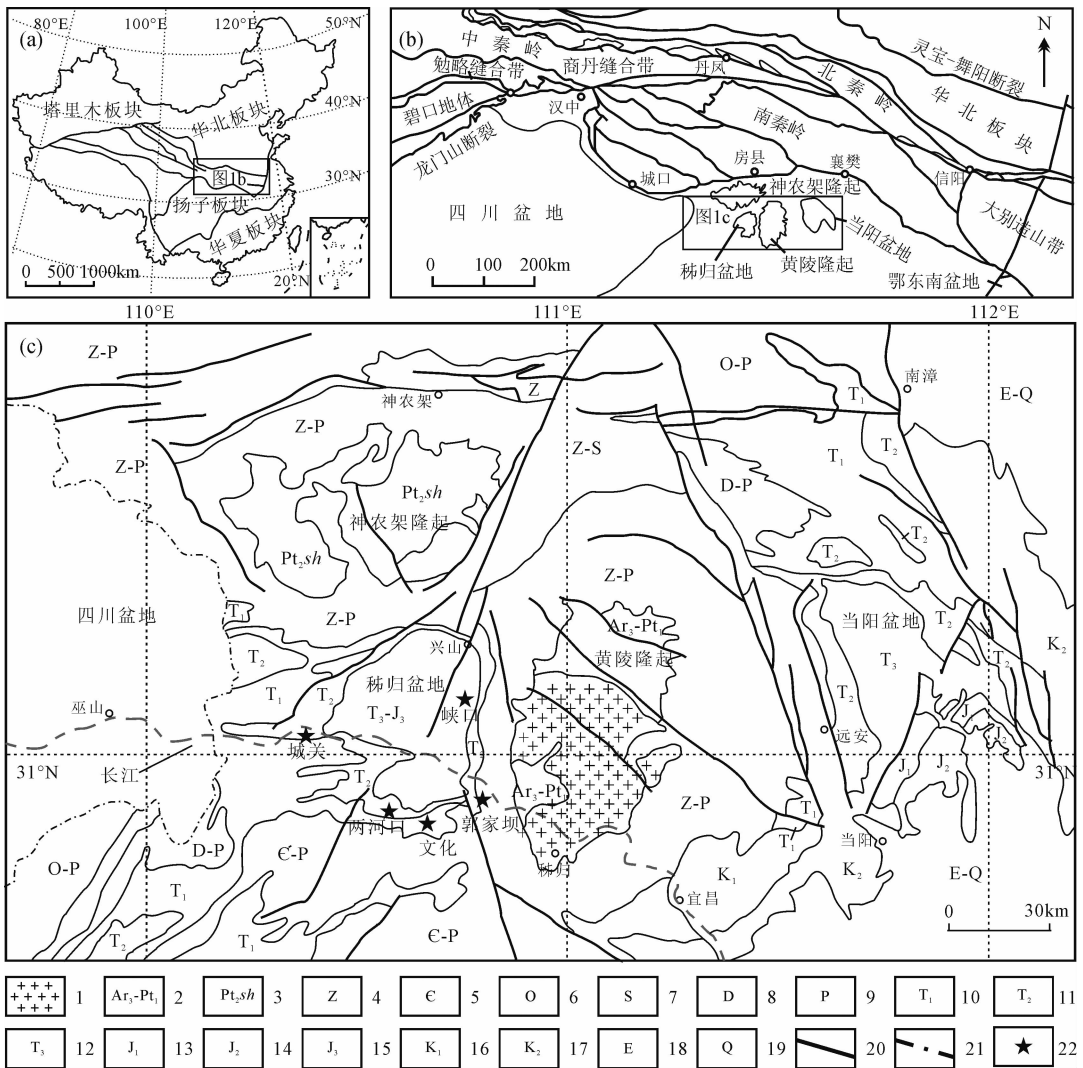


图 1 中国大陆简明地质图(a)和中扬子北缘周边构造单元分布图(b)(a, b 据 Dong Yunpeng et al., 2016; 刘少峰等, 2010 修改)及研究区简明地质图(c) (据龚志愚等, 2014 修改)

Fig. 1 Tectonic units diagram of mainland China (a) and regional geological map of north margin of Middle Yangtze (b) (a, b modified from Dong Yunpeng et al., 2016; Liu Shaofeng et al., 2010) and geological map of the studied area (c) (modified from Gong Zhiyu et al., 2014)

1—黄陵花岗岩体; 2—新太古界—古元古界; 3—中元古界神农架群; 4—震旦系; 5—寒武系; 6—奥陶系; 7—志留系; 8—泥盆系; 9—二叠系; 10—下三叠统; 11—中三叠统巴东组; 12—上三叠统九里岗组; 13—下侏罗统桐竹园组; 14—中侏罗统; 15—上侏罗统; 16—下白垩统; 17—上白垩统; 18—始新统; 19—第四系; 20—断层; 21—长江; 22—剖面

1—Huangling pluton; 2—Neoproterozoic-Paleoproterozoic; 3—Mesoproterozoic Shennongjia Group; 4—Sinian; 5—Cambrian; 6—Ordovician; 7—Silurian; 8—Devonian; 9—Permian; 10—Lower Triassic; 11—Middle Triassic Badong Formation; 12—Upper Triassic Jiuligang Formation; 13—Lower Jurassic Tongzhuyuan Formation; 14—Middle Jurassic; 15—Upper Jurassic; 16—Lower Cretaceous; 17—Upper Cretaceous; 18—Eocene; 19—Quaternary; 20—fault; 21—Yangtze River; 22—section

叠世九里岗组至晚侏罗世蓬莱镇组的陆相碎屑岩地层充填(Gong Zhiyu et al., 2014; Yu Wu et al., 2017)。巴东组是盆地的沉积基底, 主要出露于盆地的西部与南部。如在巴东城关和两河口镇(图 2a, b), 巴东组厚度超过 1000m, 各段出露相对完整, 并与下伏下三叠统嘉陵江组和上覆的上三叠统九里岗组整合接触。在盆地东部, 本组经历了不同程度的

剥蚀, 如在文化镇, 郭家坝镇等地(图 2c, d), 晚三叠世九里岗组不整合覆盖于巴东组之上, 至兴山县峡口镇一带巴东组剥蚀殆尽(图 2e)。中扬子区巴东组横向上不同程度的缺失被认为是受到晚三叠世研究区抬升和差异剥蚀(Li Xubing et al., 2008; Zhao Xiaoming et al., 2010)的影响。

巴东组具有细碎屑岩和碳酸盐岩混合沉积的宏

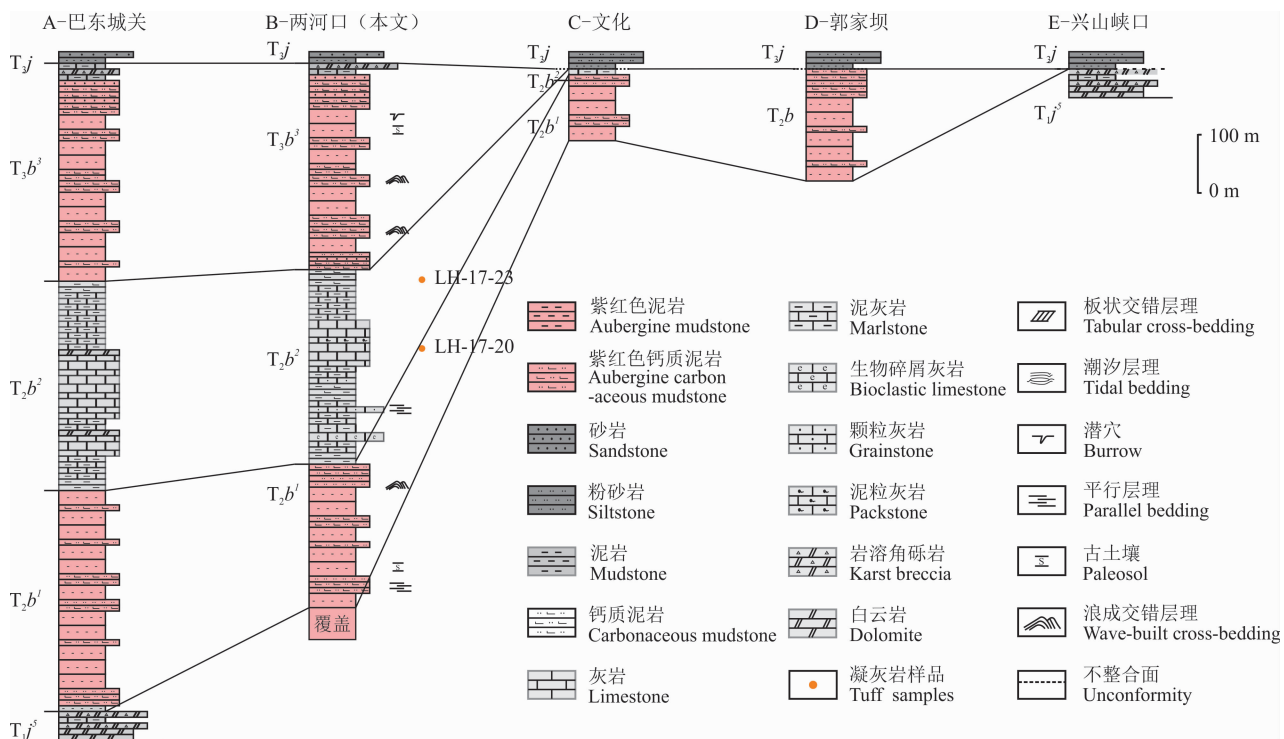


图 2 秭归盆地巴东组地层对比柱状图

Fig. 2 Stratigraphic column correlation of Badong Formation, Zigui basin

剖面 A(BGMRHP, 1996); 剖面 B(本文); 剖面 C(本文); 剖面 D(李旭兵等, 2008); 剖面 E(张震等, 2013)

Section A (湖北省地质矿产局, 1996); Section B (This study); Section C (This study);

Section D (Li Xubing et al., 2008); Section E (Zhang Zhen et al., 2013)

观特征。第一、三段岩性特征相似,以紫红色块状泥岩为主,夹细砂岩和灰绿色薄层泥岩(图 3c),发育浪成交错层理(图 3d)和水平层理(图 3e)等沉积构造。部分层位的泥岩显著古土壤化,可见潜穴(图 3f)等古土壤构造。因此认为一段代表了整体向上变细直至与泥灰岩过渡的碎屑岩潮坪序列,三段代表了另一整体向上变细的碎屑岩潮坪序列,古土壤发育程度更高。二段整体以灰色中一薄层状灰岩夹薄层状钙质泥岩为主,夹生物碎屑灰岩与颗粒灰岩(图 3g),为潮下带至局限台地沉积,代表一次规模较大的海侵事件。薄片鉴定结果显示,巴东组细砂岩主要由单晶石英、斜长石、灰岩岩屑和酸性火山岩屑(图 3h, i)组成,此外还发现了数量可观的黑云母碎屑。

凝灰岩样品 LH-17-20 和 LH-17-23 分别取自于秭归县两河口剖面巴东组二段中部与顶部(图 2b, 图 3a, b),凝灰岩为褐黄色一黄白色,呈疏松的薄层夹在厚层的泥灰岩中。

2 分析方法与结果

2.1 测试方法

将采集的共计 2 件样品进行粗碎至 2cm,随后

细碎并使用传统的磁力与重液分选手段进行分选,并在双目镜下对锆石进行逐一筛选。筛选完备后,对于砂岩样品中的碎屑锆石进行随机挑选,尽量选择凝灰岩样品中表面洁净且晶型较好的锆石,并将锆石颗粒粘接至双面胶上,固定于无色的环氧树脂中,对样品靶整体进行 1/2~1/3 程度的抛光。为更好地甄别锆石形态特征,上机测试之前对样品靶进行透-反射与阴极发光(CL)拍照,由此来确定锆石的内部特征,在测试选点的过程中避免裂隙与混合年龄的影响。

所有样品(靶)均在中国地质大学(武汉)地质过程和矿产资源国家重点实验室 LA-ICP-MS(激光剥蚀电感耦合等离子质谱仪)进行测试,实验原理是利用激光轰击(剥蚀)样品抛光表面,随后引导离子进入质谱仪分析。激光斑束直径 32μm,脉冲数 300。对于获得的信号,配合标样 NIST SRM 610(微量元素)、91500(外标)和 GJ-1(监控样)进行比对测定和校正,最后得到同位素及微量元素信号。数据处理、U-Pb 年龄计算在 ICPMSDataCal 10.9 (Liu Yongsheng et al., 2008, 2010)软件中生成。对生成的锆石 U-Pb 年龄利用 Isoplot 3.27 投图,详细过



图 3 秭归盆地巴东组的典型野外现象与岩石薄片照片

Fig. 3 Typical field phenomenon and microscopic photos of rock slices from Badong Formation, Zigui basin

(a)—巴东组中下部凝灰岩 LH-17-20; (b)—巴东组顶部凝灰岩 LH-17-23; (c)—古土壤化的块状紫红色泥岩中含有灰绿色的稳定薄层, 指示了潜水面; (d)—发育于巴东组三段的浪成交错层理; (e)—发育于巴东组二段的水平层理; (f)—巴东组三段中发育的潜穴构造; (g)—巴东组二段颗粒灰岩; (h, i)—巴东组细砂岩薄片; Q—石英; Pl—斜长石; K—钾长石; Cal—灰岩岩屑; Lv—火山岩屑(微晶, 霏细晶)

(a)—Tuff sample LH-17-20 from the Lower Badong Formation; (b)—tuff sample LH-17-23 from the top of Badong Formation; (c)—fuchsia thick-massive paleosol contains a stable greyish thin layer which indicates paleo-water table; (d)—wave-built cross-bedding of the 3rd Member of the Badong Formation; (e)—horizontal bedding of the 2nd Member of the Badong Formation; (f)—burrow structure; (g)—grain-limestone of the 2nd Member of the Badong Formation; (h, i)—fine sandstone slices; Q—quartz; Pl—plagioclase; K—K-feldspar; Cal—limestone lithic fragments; Lv—volcanic lithic fragments (microcrystalline and felsitic)

程见于 Ludwig(2003)。对于 $<1000\text{Ma}$ 的锆石, 选择 $^{206}\text{Pb}/^{238}\text{U}$ 年龄, 主要是基于 ^{235}U 半衰期短 (Jaffey et al., 1971), 相应地, ^{235}U 衰变成 ^{207}Pb 的含量低, 子体同位素丰度小, 测试相对误差大。本文采取 $^{206}\text{Pb}/^{238}\text{U}$ 样品表面年龄。

2.2 分析结果

(1) 锆石的形态学特征。锆石不仅具有复杂的成因与广泛的来源, 而且往往具有多期生长或区域重置的复杂内部结构 (Corfu et al., 2003), 微区原位定年 (in situ) 可以得到锆石不同区域的多组年龄。因此, 通过阴极发光图像 (CL) 以及锆石微量元素等手段对锆石进行成因分类是合理解释年龄数据的第一步。来自凝灰岩夹层的锆石颗粒多呈无色至淡黄绿色, 晶形常为半自形至自形。LH-17-20 部分

锆石呈现粒状, 粒径多在 $50\sim 70\mu\text{m}$ 之间, 磨圆程度很小, 其余颗粒与样品 LH-17-23 均为为典型的长柱状至针状, 柱长多在 $150\mu\text{m}$ 以上, 外形完整, 无磨圆, 指示锆石没有经历搬运过程。绝大多数锆石的 CL 照片显现出明显的振荡环带 (图 4)。

(2) 锆石地球化学特征。两件样品的 Th/U 比值均大于 0.4, 大多数样品表现为强烈的 δCe 正异常, δEu 的负异常和 HREE 富集 (图 5), ΣREE 值较大等特点。综合上述特征以及镜下发现的酸性火山岩屑, 认为锆石为岩浆成因。岩浆锆石的 Hf 以及 Ti 含量可以反映岩浆分异度的大小, 所分析锆石颗粒 Hf 含量中等—高 ($8085\times 10^{-6}\sim 11263\times 10^{-6}$), 利用锆石 Ti 温度计 (Watson et al., 2006) 得出样品的结晶温度介于 $595\sim 763\text{C}$ 之间, 因此认为锆石

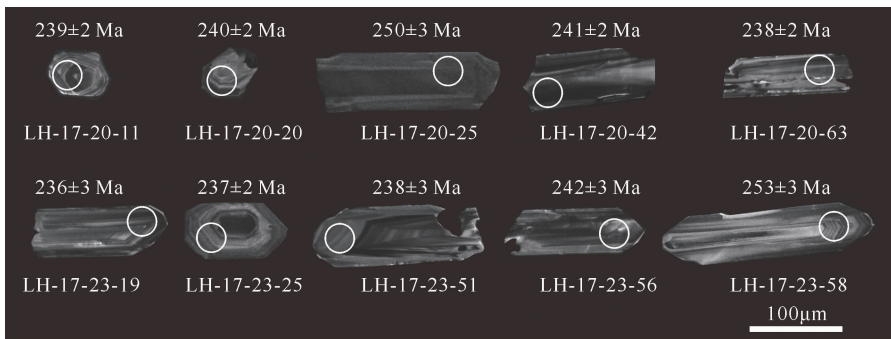


图4 秭归盆地巴东组凝灰岩锆石阴极发光照片与激光点阵

Fig. 4 CL images and laser spots of zircons from tuff of Badong Formation in Zigui basin

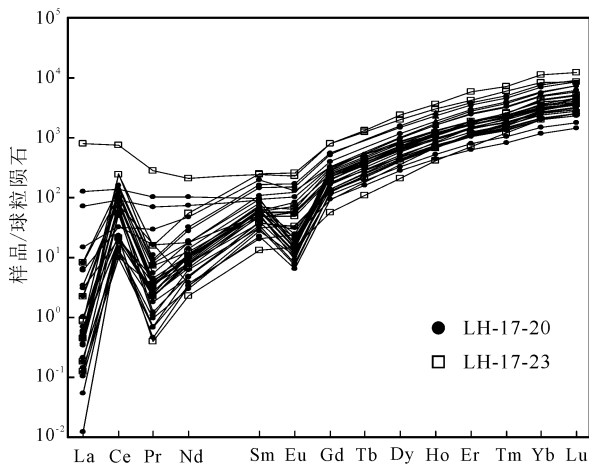


图5 秭归盆地巴东组凝灰岩锆石稀土元素球粒陨石标准化配分图(球粒陨石标准化值据 Sun et al., 1989)

Fig. 5 Chondrite-normalized REE curve of zircons from tuffs of Badong Formation in Zigui basin (standardized value according to Sun et al., 1989)

结晶于分异度较高的酸性岩浆。Th/U-Nb/Hf 和 Th/Nb-Hf/Th 图解(Yang Jianghai et al., 2012) 表明,绝大多数锆石应源自与造山或弧相关的岩浆

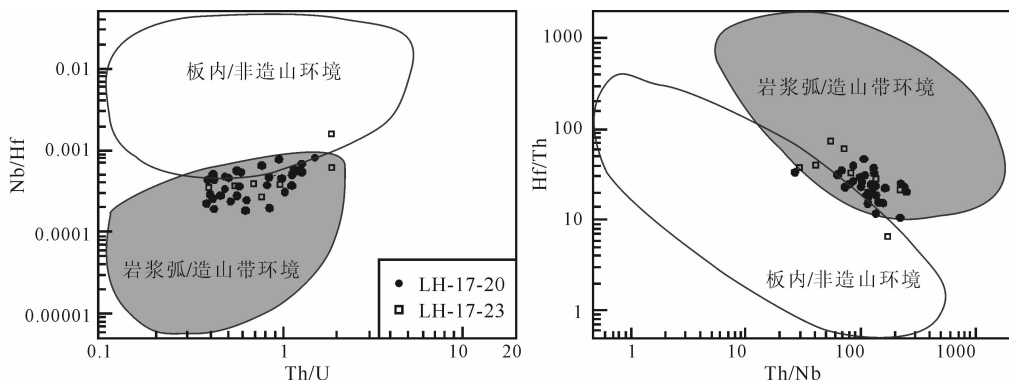


图6 秭归盆地巴东组锆石 Th/U-Nb/Hf 和 Th/Nb-Hf/Th 图解(据 Yang Jianghai et al., 2012 修改)

Fig. 6 Th/U-Nb/Hf and Th/Nb-Hf/Th discrimination diagram of zircons in tuff of Badong Formation in Zigui basin (modified from Yang et al., 2012)

结晶作用(图6)。

2.3 锆石 U-Pb 年龄

巴东组二段凝灰岩样品 LH17-20 和 LH17-23 锆石 U-Pb 同位素定年结果见表2。样品 LH-17-20 具有 27 颗较谐和的锆石(谐和度 $\geq 90\%$,图7a),它们的 $^{206}\text{Pb}/^{238}\text{U}$ 年龄介于 $236.7 \pm 2\text{Ma}$ 至 $263 \pm 3\text{Ma}$ 之间,在 U-Pb 年龄分布直方图中显示出 241Ma 和 251Ma 两个明显峰值(图7b)。对于较年轻的 $\sim 241\text{Ma}$ 峰值,其 $^{206}\text{Pb}/^{238}\text{U}$ 加权平均年龄为 $241.7 \pm 1.7\text{Ma}$ ($n=7$, MSWD=1.15)(图7a),代表了最新一期火山喷发或是凝灰岩在地层中的就位年龄。 $\sim 251\text{Ma}$ 的峰值指示了早期岩浆结晶或是火山喷发的年龄。

样品 LH-17-23 具有 8 颗较谐和的锆石(图7c),它们的 $^{206}\text{Pb}/^{238}\text{U}$ 年龄大多介于 $236.8 \pm 2\text{Ma}$ 至 $241 \pm 3\text{Ma}$ 之间,在 U-Pb 年龄分布直方图中主要显示出 237Ma 一期峰值(图7d)。样品 LH-17-23-16 和 LH-17-23-58 年龄偏大一些,分别为 $248 \pm 3.5\text{Ma}$ 和 $253 \pm 2.8\text{Ma}$ 。样品主年龄峰的 $^{206}\text{Pb}/^{238}\text{U}$ 加权年龄为 $237.5 \pm 2\text{Ma}$ ($n=6$, MSWD=0.42)

表 2 秭归盆地巴东组二段凝灰岩样品 LH17-20 和 LH17-23 锆石 U-Pb 同位素定年结果
Table 2 Zircon U-Pb chronological dating results of tuff sample LH17-20 & LH17-23 from the 2nd Member of Badong Formation

测点	$(\times 10^{-6})$		同位素比值						同位素年龄(Ma)						谐和度	
	Th	U	$^{207}\text{Pb}/^{209}\text{Pb}$	$^{207}\text{Pb}/^{235}\text{U}$	$^{206}\text{Pb}/^{238}\text{U}$	1σ	$^{207}\text{Pb}/^{206}\text{Pb}$	1σ	$^{207}\text{Pb}/^{235}\text{U}$	1σ	$^{206}\text{Pb}/^{238}\text{U}$	1σ	$^{207}\text{Pb}/^{235}\text{U}$	1σ	$^{206}\text{Pb}/^{238}\text{U}$	1σ
LH17-20-1	449.5638	1005.0324	0.0517	0.0014	0.0078	0.0004	0.2914	0.0406	0.0004	272.2850	62.9550	259.6881	6.1436	256.5870	2.2343	98%
LH17-20-2	401.3561	1065.5967	0.0527	0.0014	0.0075	0.0003	0.2908	0.0397	0.0003	322.2800	59.2525	259.1657	5.9037	250.7745	2.0521	96%
LH17-20-3	364.6754	752.0323	0.0533	0.0015	0.0087	0.0004	0.3043	0.0411	0.0004	338.9450	66.6600	269.7759	6.7453	259.5049	2.2884	96%
LH17-20-6	237.7582	568.1903	0.0518	0.0020	0.0102	0.0004	0.2880	0.0404	0.0004	275.9900	87.0225	256.9563	8.0559	255.3949	2.4689	99%
LH17-20-7	654.8559	1242.3147	0.0513	0.0016	0.0083	0.0004	0.2788	0.0392	0.0004	253.7700	65.7300	249.6846	6.5988	247.6943	2.3924	99%
LH17-20-8	314.7619	839.6333	0.0527	0.0020	0.0107	0.0004	0.2913	0.0398	0.0004	316.7250	117.5800	259.5902	8.4166	251.7633	2.4771	96%
LH17-20-9	420.8692	891.7389	0.0535	0.0018	0.0094	0.0004	0.2890	0.0391	0.0004	350.0550	49.9950	257.7779	7.4298	247.2946	2.2011	95%
LH17-20-11	409.5948	746.8377	0.0519	0.0017	0.0088	0.0003	0.2716	0.0379	0.0003	279.6900	71.2875	243.9777	7.0045	239.9008	1.8894	98%
LH17-20-13	411.5963	676.7230	0.0528	0.0017	0.0092	0.0003	0.2866	0.0392	0.0003	320.4300	69.4375	255.8743	7.2381	248.8011	1.9863	97%
LH17-20-15	521.4959	1166.1011	0.0502	0.0013	0.0075	0.0003	0.2762	0.0398	0.0003	211.1850	61.1000	247.6251	5.9352	251.5292	2.1396	98%
LH17-20-16	389.3289	1116.4978	0.0546	0.0017	0.0096	0.0004	0.3117	0.0414	0.0004	394.4950	68.5125	275.4628	7.4017	261.2343	2.2754	94%
LH17-20-20	660.7500	1172.3647	0.0536	0.0015	0.0077	0.0003	0.2821	0.0380	0.0003	353.7600	64.8075	252.3299	6.1307	240.6807	1.9237	95%
LH17-20-22	361.8733	1022.2789	0.0530	0.0016	0.0091	0.0004	0.2931	0.0397	0.0004	327.8350	68.5125	260.9600	7.1831	250.8422	2.3219	96%
LH17-20-24	506.4106	1325.3517	0.0550	0.0019	0.0382	0.0005	0.3082	0.0403	0.0005	413.0100	77.7700	272.7496	8.1245	254.6885	2.8121	93%
LH17-20-25	484.8537	912.5852	0.0524	0.0022	0.0119	0.0005	0.2888	0.0397	0.0005	301.9100	91.6550	257.6483	9.4012	250.6919	2.8512	97%
LH17-20-27	368.9930	735.1858	0.0553	0.0021	0.0107	0.0004	0.2966	0.0387	0.0004	433.3800	80.5475	263.7049	8.3630	244.9209	2.3782	92%
LH17-20-28	295.7451	861.4380	0.0563	0.0019	0.0350	0.0004	0.3250	0.0416	0.0004	464.8600	75.9175	285.7676	8.4012	262.5185	2.7532	91%
LH17-20-32	455.4995	338.1411	0.0558	0.0027	0.0392	0.0005	0.3092	0.0402	0.0005	455.6000	109.2475	273.5648	11.6401	253.8459	2.7970	92%
LH17-20-33	898.6478	447.9041	0.0547	0.0024	0.0122	0.0004	0.2921	0.0389	0.0004	398.2000	98.1375	260.2360	9.5498	245.7109	2.5900	94%
LH17-20-34	391.7745	326.2753	0.0560	0.0028	0.0366	0.0005	0.3166	0.0410	0.0005	453.7500	113.8775	279.2659	11.7572	259.2406	3.1138	92%
LH17-20-36	300.5571	367.0382	0.0548	0.0024	0.0309	0.0004	0.3059	0.0404	0.0004	466.7100	96.2875	270.9696	9.8841	255.1530	2.6373	93%
LH17-20-40	257.9760	265.4376	0.0507	0.0032	0.0183	0.0005	0.2904	0.0418	0.0005	233.4000	143.5000	258.8816	14.3979	263.7326	3.0546	98%
LH17-20-42	393.4888	393.0664	0.0495	0.0026	0.0137	0.0004	0.2609	0.0381	0.0004	172.3050	128.6850	235.3919	11.0328	241.0870	2.4189	97%
LH17-20-45	614.5309	457.0731	0.0555	0.0022	0.03078	0.0004	0.3078	0.0403	0.0004	431.5300	88.8800	272.4891	9.5399	254.9261	2.7840	93%
LH17-20-61	211.2967	249.0965	0.0530	0.0032	0.0173	0.0004	0.2845	0.0386	0.0004	327.8350	135.1650	254.2372	13.6997	244.3003	2.7803	96%
LH17-20-63	513.0863	404.0788	0.0535	0.0023	0.0115	0.0004	0.2780	0.0377	0.0004	350.0550	96.2875	249.0666	9.1728	238.7686	2.3146	95%
LH17-20-64	271.5485	357.8881	0.0525	0.0025	0.0130	0.0004	0.2800	0.0387	0.0004	309.3200	107.3900	250.6853	10.3325	244.5853	2.4991	97%
LH17-23-16	323.0807	306.2670	0.0521	0.0016	0.0082	0.0006	0.2788	0.0392	0.0006	300.0600	73.1400	249.7323	6.5002	248.1040	3.5207	99%
LH17-23-19	356.5139	305.2265	0.0516	0.0017	0.0087	0.0004	0.2653	0.0374	0.0004	333.3900	75.9150	238.9151	6.9704	236.8550	2.7108	99%
LH17-23-22	1504.0751	752.6829	0.0555	0.0011	0.0063	0.0004	0.2880	0.0374	0.0004	435.2300	42.5900	256.9956	5.0056	236.7805	2.2734	91%
LH17-23-25	477.9074	407.8063	0.0505	0.0012	0.0059	0.0003	0.2602	0.0374	0.0003	216.7400	52.7675	234.8077	4.7187	236.8198	1.7846	99%
LH17-23-51	731.0244	448.7550	0.0520	0.0018	0.0093	0.0004	0.2698	0.0376	0.0004	287.1000	76.8425	242.5488	7.4223	238.0994	2.5961	98%
LH17-23-52	197.2239	234.4871	0.0561	0.0043	0.0180	0.0007	0.2778	0.0375	0.0007	453.7500	170.3475	248.9331	14.3285	237.1140	4.6445	95%
LH17-23-56	140.8342	235.0468	0.0532	0.0027	0.0145	0.0005	0.2811	0.0382	0.0005	344.5000	119.4300	251.5133	11.5048	241.6977	3.1813	96%
LH17-23-58	253.4804	250.7814	0.0540	0.0025	0.0133	0.0005	0.2969	0.0401	0.0005	368.5700	106.4700	263.9799	10.4153	253.5256	2.8232	95%

(图7c)。这一年龄代表了巴东组二段顶部凝灰岩的就位(沉积)年龄。

3 讨论

3.1 巴东组的地层时代

在上扬子区嘉陵江组顶部,巴东组或是雷口坡组底部发育了一套沉凝灰岩(“绿豆岩”),长期以来被视为中上三叠统的划分标志(四川省地质矿产局,1997),其中的碎屑锆石给出了246Ma的最小峰值(Sun Yan et al., 2017)。而在湖北省利川以东,巴东组底部不发育绿豆岩,主要依据中三叠世早期的双壳类组合 *Eumorphotis (Asoella) subillyrica*-*Myophoria (Costatoria) goldfussi mansuyi* 等(张振来等,1987;汪啸风等,2002)确定地层年代。由此可见巴东组底部的沉积时限应为中三叠世早期。巴东组一、二段发育菊石、双壳类、牙形石等多门类化石。双壳类以 *Myophoria (Costatoria) goldfussi*、*Leptochondria illyrica* 和 *L. subillyrica* 等为特征,其中后两者在我国中三叠世早期出现并开始繁盛,并上延到拉丁期(湖北省地质矿产局,1990)。菊石类则以出露于利川以西巴东组二段的 *Progonoceratites* 菊石动物群为代表,时代归属安尼

晚期(Yang Zunyi et al., 1982)或拉丁早期(张振来等,1987)。此外,一、二段还含有植物 *Pleuromeia marginulata-Annalepis zeilleri* 组合(Zhou Tongshun et al., 1985; Sun Ge et al., 1995),孢粉 *Lundbladispora neburgii-Alatisporites furongqiaoensis* 组合(Qu Lifan et al., 1983),以 *Neospathodus kockeli* 为主的牙形石组合,以 *Glomospira nanzhangensis* 组合为代表的有孔虫和 *Xiangxiella* 叶肢介动物群等,以上化石的时代(湖北省地质矿产局,1996)大多归属于安尼期,部分延续到拉丁期。发育于巴东组二段中部的凝灰岩样品 LH-17-20 最小年龄峰的加权平均年龄为 241.7 ± 1.7 Ma,佐证了上述生物化石记录表明巴东组一、二段应沉积于中三叠世安尼期至拉丁期。

巴东组三段化石记录较少,化石延限较长,安尼期繁盛的 *Pleuromeia* 植物和 *Lundbladispora* 孢子(Li Xingxue et al., 1995)在该段中已不复存在(汪啸风等,2002),*Costatoria goldfussi* 和 *Scyehentolium cf. kokeni* 等兼具中、晚三叠世的分子(张振来等,1987)被保留。Meng Fansong et al. (2003)在巴东组三段发现了多种具有中三叠世晚期向晚三叠世早期过渡色彩的植物化石,如

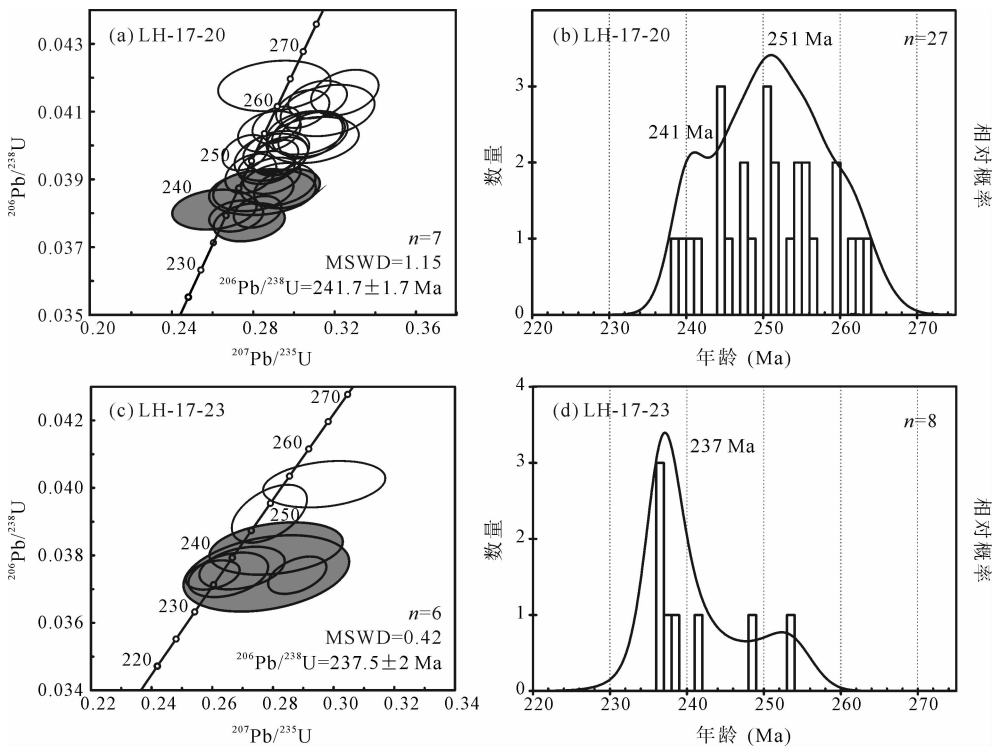


图7 秭归盆地巴东组凝灰岩锆石 U-Pb 年龄谐和图(a, c)和频率分布直方图(b, d)

Fig. 7 U-Pb concordia diagram (a, c) and U-Pb age distribution and probability density plots histograms (b, d) of zircons from tuff samples of Badong Formation in Zigui basin

Annalepis latiloba Meng、*Equisetites arenaceus* (Jaeger)、*Scytophyllum* sp. 等。本文报道的巴东组二段顶部样品 LH-17-23 主年龄峰给出了 $237.5 \pm 2\text{Ma}$ 的加权平均年龄,代表了火山喷发的年龄或凝灰岩在沉积地层中的就位时代,这一年龄亦是国际地层委员会推荐拉丁期与卡尼期的界线(Mietto et al., 2012)。此外,考虑到巴东组在研究区西部各段发育良好且与上覆晚三叠世九里岗组整合接触(图 2A),如果将巴东组的顶界归入安尼阶或是拉丁阶中下部,那么上覆的九里岗组也将下延到中三叠统,这显然是不合适的。综上所述,凝灰岩夹层与化石记录综合表明巴东组三段应晚于 $\sim 237\text{Ma}$ 沉积,巴东组的地层时代跨越整个中三叠世,并进入晚三叠世早期。

3.2 地质意义

凝灰岩层的定年结果结合生物化石记录很好地约束了巴东组的地层时代,这一发现具有两点地质意义。

首先,凝灰岩的发现有助于进一步地理解印支运动对研究区的具体影响。传统学术观点认为,巴东组整体代表了中三叠世安尼期研究区整体微弱抬升,海水变浅,是对印支运动 I 幕的沉积响应(Li Xubing et al., 2008; Zhao Xiaoming et al., 2010); 顶部与九里岗组的不整合面代表了长期的沉积间断,被视为对研究区北部秦岭造山带碰撞造山事件的响应(Chai Rong et al., 2016),对应印支运动 II 幕。本文报道的巴东组凝灰岩夹层丰富了上述认识。第一,巴东组二段中数层凝灰岩和细砂岩中的火山岩屑证实了中三叠世研究区周边多期火山活动的存在。凝灰岩中造山型微量元素特征的岩浆锆石表明火山活动可能与研究北部秦岭造山带的碰撞造山事件有关(Zhang Guowei et al., 1996, 2003; Hu Fangyang et al., 2017)。另外,巴东组细砂岩中含有石英、黑云母碎屑和以灰岩、白云岩为主的沉积岩屑。由此可见,印支运动 I 幕对于研究区的影响不仅表现为区域抬升作用,也反映了活动背景源区对于研究区的初期碎屑供给。第二,针对巴东组的沉积学研究 and 凝灰岩层定年结果表明,巴东组二段陆棚相灰岩向三段滨海潮坪相泥岩的过渡代表了中晚三叠世之交海水大规模退去的节点,随后晚三叠世早—中期,印支运动 II 幕启动,研究区抬升和差异剥蚀,造成了巴东组横向上不同程度的缺失,标志着秭归盆地开始向陆相前陆盆地体系演化(Liu Shaofeng et al., 2005, 2010, 2015)。

其次,巴东组年代框架的确立为上、中扬子区“最高海相层”的对比奠定了基础,对于追溯印支期上、中扬子区大规模海退历史具有指示意义。“最高海相层”被定义为某一地区海相沉积结束时的沉积地层,由此之上再无海相沉积出现(Beck et al., 1995; Rage et al., 1995)。巴东组是鄂西地区的“最高海相层”,由二段陆棚相灰岩至三段滨岸潮坪泥岩的转变代表了本区印支期大规模海退的起点(Li Xubing et al., 2008),凝灰岩层定年结果将其限定为中晚三叠世之交。在研究区东部的鄂东南地区,陆水河组代表了残留海湾的灰泥质沉积(Tong Jinnan, 2015),时代被归入中三叠世安尼阶(Tong Jinnan et al., 2018);而在川东至川西一线,残留的、最新的海相灰岩地层以晚三叠世卡尼期马鞍塘组(Mei Mingxiang, 2014)为代表。由此可见,上、中扬子区大规模海退的启动时间存在较大的差异,这种穿时性特征也印证了由中三叠世安尼期晚期至晚三叠世卡尼期海水大规模向西退去的特征(刘宝珺等, 1994; Liu Zhili et al., 2001; 马永生等, 2009)。

4 结论

新发现于宜昌市秭归县两河口地区的巴东组二段顶部的凝灰岩夹层给出了 $237.5 \pm 3.1\text{Ma}$ 的加权平均年龄,代表了凝灰岩夹层的就位时代。这一年龄结合生物化石记录较好地约束了巴东组的地层年代为中三叠世安尼期至晚三叠世早期。凝灰岩层、造山型微量元素特征的锆石和巴东组的沉积学特征反映了活动背景的源区对于中扬子区的初始碎屑供给,代表了中扬子区对印支运动的沉积响应。以巴东组为代表的“最高海相层”穿时地分布于鄂东南至川西一线,反映了上、中扬子区由中三叠世安尼期晚期至晚三叠世卡尼期海水大规模向西退去的特征。

致谢:审稿专家的建议使本文增色良多,特此感谢。

References

- Beck R A, Burbank D W, Sercombe W J, Riley G W, Barndt J K, Berry J R, Afzal J, Khan A M, Jurgen H, Metje J, Cheema A, Shafique N A, Lawrence R D, Khan M A. 1995. Stratigraphic evidence for an early collision between northwest India and Asia. *Nature*, 373(6509): 55.
- Bo Jingfang, Yao Jianxin, Lin Baoyu, Liu Weiqing, Li Ming. 2019. Distribution and age of the Triassic marinered beds in eastern Sichuan and Chongqing. *Acta Geologica Sinica*, 93(2): 285~301 (in Chinese with English abstract).
- Chai Rong, Yang Jinghai, Du Yuansheng, Ding Dianshi. 2016. Middle Triassic-Early Jurassic sedimentary record in the Zigui

- basin and implication for the Qinling Indosinian collisional orogens. *Geological Science and Technology Information*, 35(4):43~49 (in Chinese with English abstract).
- Corfu F, Hanchar J M, Hoskin P W O, et al. 2003. Atlas of zircon textures. *Reviews in Mineralogy & Geochemistry*, 53(1):469~500.
- Dong Yunpeng, Zhang Guowei, Neubauer F, Liu Xiaoming, Gensor J, Hauzenberger C. 2011. Tectonic evolution of the Qinling orogen, China: review and synthesis. *Journal of Asian Earth Sciences*, 41(3):213~237.
- Dong Yunpeng, Santosh M. 2016. Tectonic architecture and multiple orogeny of the Qinling orogenic belt, Central China. *Gondwana Research*, 29(1):1~40.
- Gong Zhiyu, Zhang Hanjin, Li Zhonglin, Luo Hong, Luo Fan, Liu Li, Du Lichao, Pan Longke. 2014. Sedimentology and evolution history of Zigui basin. *Resource Environment & Engineering*, 4(28): 35~39 (in Chinese with English abstract).
- Hu Fangyang, Ducea M N, Liu Shuwen, Chapman J B. 2017. Quantifying crustal thickness in continental collisional belts: global perspective and a geologic application. *Scientific Reports*, 7(1):7058.
- Huang Hu, Yang Jianghai, Du Yuansheng, Huang Hongwei, Huang Zhiqiang, Xie Chunxia, Hu Lisha. 2012. LA-ICPMS U-Pb dating of zircons from tuffs of the Upper Permian-Middle Triassic in Youjiang basin, Guangxi Province and its geological significance. *Journal of Earth Science*, 37(1): 125~138 (in Chinese with English abstract).
- Jaffey A H, Flynn K F, Glendenin L E, Bentley W C, Essling A M. 1971. Precision measurement of half-lives and specific activities of U 235 and U 238. *Physical Review C*, 4(5):1889.
- Li Xingxue, Zhou Zhiyan, Cai Chongyang. 1995. Flora in Geological History of China. Guangzhou: Guangdong Science and Technology Press, 229~259 (in Chinese without English abstract).
- Li Xubing, Wang Chuanshang, Liu An. 2008. Sedimentary response to the Indosinian movement—a case study of the Mid-Upper Triassic in the Zigui basin, Hubei. *Geology in China*, 35(5): 984~991 (in Chinese with English abstract).
- Liu Shaofeng, Steel R, Zhang Guowei. 2005. Mesozoic sedimentary basin development and tectonic implication, northern Yangtze Block, eastern China: record of continent-continent collision. *Journal of Asian Earth Sciences*, 25(1):9~27.
- Liu Shaofeng, Wang Ping, Hu Mingqing, Gao Tangjun, Wang Kai. 2010. Evolution and geodynamic mechanism of basin-mountain systems in the northern margin of the Middle-Upper Yangtze. *Earth Science Frontiers*, 17(3): 14~26 (in Chinese with English abstract).
- Liu Shaofeng, Qian Tao, Li Wangpeng, Dou Guoxing, Wu Peng. 2015. Oblique closure of the northeastern Paleo-Tethys in central China. *Tectonics*, 34(3):413~434.
- Liu Yongsheng, Hu Zhaochu, Gao Shan, Gunther D, Xu J, Gao Changgui, Chen Haihong. 2008. In situ analysis of major and trace elements of anhydrous minerals by LA-ICP-MS without applying an internal standard. *Chemical Geology*, 257(1~2): 34~43.
- Liu Yongsheng, Hu Zhaochu, Zong Keqing, Gao Changgui, Gao Shan, Xu Juan, Chen Haihong. 2010. Reappraisal and refinement of zircon U-Pb isotope and trace element analyses by LA-ICP-MS. *Chinese Science Bulletin*, 55(15):1535~1546.
- Ludwig K R. 2003. User's manual for isoplot 3.00, a geochronological toolkit for microsoft excel. Berkeley Geochronol. Cent. Spec. Publ., 4:25~32.
- Macdonald F A, Schmitz M D, Crowley J L, et al. 2010. Calibrating the Cryogenian. *Science*, 327(5970): 1241~1243.
- Mei Mingxiang. 2014. The sequence-stratigraphic framework of the Late Triassic in the Upper Yangtze region, South China; stratigraphic forcing for the death of the Yangtze platform and the birth of the Upper-Yangtze foreland basin. *Acta Geologica Sinica*, 88(10): 1944~1969.
- Meng Fansong, Li Xubing. 2003. Meticulous correlation of Upper Triassic Series on the eastern and western limbs of the Huangling dome, western Hubei. *Geology and Mineral Resources of South China*, 4: 60~65 (in Chinese without English abstract).
- Mietto P, Manfrin S, Preto N, Rigo M, Roghi G, Furin S, Gianolla P, Posenato P, Muttoni G, Nicora A, Buratti N, Cirilli S, Spoet C, Ramezani J, Bowring S A. 2012. The Global Boundary Stratotype Section and Point (GSSP) of the Carnian Stage (Late Triassic) at Prati di Stuares/Stuares Wiesen Section (Southern Alps, NE Italy). *Episodes*, 35: 414~430.
- Qian Tao, Liu Shaofeng, Wang Zongxiu, Li Wangpeng, Chen Xinlu. 2016. A detrital record of continent-continent collision in the Early-Middle Jurassic foreland sequence in the northern Yangtze foreland basin, South China. *Journal of Asian Earth Sciences*, 131:123~137.
- Qu Lifan, Yang Jiduan, Bai Yunhong, Zhang Zhenlai. 1983. Characteristics of palynological assemblage of Triassic China and a preliminary probe into partitions. *Journal of the Chinese Academy of Geological Sciences*, 5: 81~94.
- Rage J C, Cappetta H, Hartenberger J L, Jaeger J J, Sudre J, Vianey-Liaud M, Kumar K, Prasad G V R, Sahni A. 1995. Collision age. *Nature*, 375(6529): 286.
- Richthofen F V. 1912. China III. Berlin.
- Shao Tongbin, Cheng Nanfei, Song Maoshuang. 2016. Provenance and tectonic-paleogeographic evolution: Constraints from detrital zircon U-Pb ages of Late Triassic-Early Jurassic deposits in the northern Sichuan basin, central China. *Journal of Asian Earth Sciences*, 127:12~31.
- Sun S S, McDonough W F. 1989. Chemical and isotopic systematics of oceanic basalts: implications for mantle composition and processes. *Geological Society London Special Publications*, 42(1):313~345.
- Sun Yan, Gao Yun, Wang Denghong, Dai Hongzhang, Gu Wenshuai, Li Jian, Zhang Lihong. 2017. Zircon U-Pb dating of 'mung bean rock' in the Tongliang area, Chongqing and its geological significance. *Rock and Mineral Analysis*, 36(6): 649~658 (in Chinese with English abstract).
- Tong Jinnan. 2015. Division and correlation of marine Lower-Middle Triassic strata in East China. *Acta Geoscientia Sinica*, 36(5): 546~558 (in Chinese with English abstract).
- Tong Jinnan, Chu Daoliang, Liang Lei, Shu Wenchao, Song Haijun, Song Ting, Song Huyue, Wu Yuyang. 2018. Triassic integrative stratigraphy and timescale of China. *Science China Earth Sciences*, 48: 1~33 (in Chinese with English abstract).
- Wang Xiaofeng, Chen Xiaohong, Zhang Renjie. 2002. Protection of Precious Geological Remains in the Yangtze Gorges Area, China with Study of the Archean-Mesozoic Multiple Stratigraphic Subdivision and Sea-Level Change. Beijing: Geological Publishing House, 240~252 (in Chinese with English abstract).
- Wang Yuejun, Fan Weiming, Zhang Guowei, Zhang Yanhua. 2013. Phanerozoic tectonics of the South China Block; key observations and controversies. *Gondwana Research*, 23(4): 1273~1305.
- Wang Zunzhou, Tian Chuanrong, Yang Xianhe, Li Jinhua, Ding Baoliang. 1992. Triassic Multi-Stratigraphic multiple division and correlation of South China. *Bulletin of the Chengdu Institute of Geology and Mineral Resources, The Chinese Academy of Geological Sciences* (in Chinese with English abstract).
- Watson E B, Wark D A, Thomas J B. 2006. Crystallization thermometers for zircon and rutile. *Contributions to Mineralogy & Petrology*, 151(4):413.
- Xie Jiarong, Zhao Yazeng. 1925. Mesozoic strata in the Yangtze River valley. *Bulletin of the Geological Society of China*, 4(1): 45~52 (in Chinese with English abstract).
- Xu Deyou. 1938. New material for Triassic fossils in South China.

- Geological Review, 4(5): 1~20 (in Chinese without English abstract).
- Yang Jianghai, Cawood P A, Du Yuansheng, Huang Hu, Hu Lisha. 2012. Detrital record of Indosinian Mountain building in SW China: Provenance of the Middle Triassic turbidites in the Youjiang Basin. *Tectonophysics*, 574~575(11):105~117.
- Yang Zunyi, Li Zishun, Qu Lifan. 1982. The Triassic system of China. *Acta Geologica Sinica*, 1: 1~20 (in Chinese with English abstract).
- Yang Zunyi, Zhang Shunxin, Yang Jiduan, Zhou Huiqin, Cao Hongsheng. 2000. Stratigraphic code of China-Triassic. Beijing: Geological Publishing House, 29~30 (in Chinese without English abstract).
- Yu Wu, Shen Chuanbo, Yang Chaoqun. 2017. Constraints of fission track dating on the Mesozoic-Cenozoic tectonic-thermal evolution of the Zigui Basin. *Earth Science Frontiers*, 24(3): 116~126 (in Chinese with English abstract).
- Zhang Guowei, Meng Qingren, Yu Zaiping, Sun Yong, Zhou Dingwu, Guo Anlin. 1996. Orogenic process and kinetics features of Qinling Orogenic Belt. *Science in China: Earth Science*, 26(3): 193~200 (in Chinese with English abstract).
- Zhang Guowei, Dong Yunpeng, Lai Shaocong. 2003. Mianlue tectonic zone and Mianlue suture zone on southern margin of Qinling-Dabie orogenic belt. *Science in China (Series D)*, 33(12): 1121~1135 (in Chinese with English abstract).
- Zhao Xiaoming, Tong Jinnan, Yao Huazhou, Tian Yang. 2010. Sedimentary response to the Indosinian Movement in Three Gorges area. *Journal of Paleogeography*, 12(2): 177~184 (in Chinese with English abstract).
- Zhou Tongshun, Zhou Huiqin. 1985. Triassic Non-marine strata and flora of China. *Bulletin Chinese Acad. Geol. Sci.*, 5: 95~111 (in Chinese with English abstract).
- 刘宝珺, 许效松, 夏文杰. 1994. 中国南方岩相古地理图集. 北京: 科学出版社.
- 刘少峰, 王平, 胡明卿, 郜瑛郡, 王凯. 2010. 中、上扬子北部盆-山系统演化与动力学机制. *地学前缘*, 17(3):14~26.
- 梅冥相. 2014. 上扬子地区晚三叠世层序地层格架: 扬子地台消亡与上扬子前陆盆地形成的地层学效应. *地质学报*, 88(10): 1944~1969.
- 马永生, 陈洪德, 王国力. 2009. 中国南方构造-层序岩相古地理图集. 北京: 科学出版社, 150~160.
- 孟繁松, 李旭兵. 2003. 黄陵穹隆东, 西两翼上三叠统的精细对比. *华南地质与矿产*, 4: 60~65.
- 曲立范, 杨基端, 白云洪, 张振来. 1983. 中国三叠纪孢粉组合特征及其分区的初步探讨. *中国地质科学院院报*, 5: 81~94.
- 四川省地质矿产局. 1997. 全国地层多重划分对比研究, 四川省岩石地层. 武汉: 中国地质大学出版社, 256~258.
- 孙艳, 高允, 王登红, 代鸿章, 顾文帅, 李建, 张丽红. 2017. 重庆铜梁地区“绿豆岩”中碎屑锆石 U-Pb 年龄及其地质意义. *岩矿测试*, 36(6): 649~658.
- 童金南. 2015. 华东地区早一中三叠世海相地层划分和对比. *地球学报*, 36(5): 546~558.
- 童金南, 楚道亮, 梁蕾, 舒文超, 宋海军, 宋婷, 宋虎跃, 吴玉祥. 2018. 中国三叠纪综合地层和时间框架. *中国科学: 地球科学*, 48: 1~33.
- 汪啸风, 陈孝红, 张仁杰. 2002. 长江三峡地区珍贵地质遗迹保护和太古宙-中生代多重地层划分与海平面升降变化. 北京: 地质出版社, 240~252.
- 王尊周, 田传荣, 杨贤河, 李金华, 丁保良. 1992. 中国南方三叠纪地层多重划分对比. *中国地质科学院成都地质矿产研究所刊*.
- 谢家荣, 赵亚曾. 1925. 扬子江峡谷的中生代地层. *中国地质学会志*, 4(1): 45~52.
- 许德佑. 1938. 中国南部三叠纪化石之新材料. *地质论评*, 4(5): 1~20.
- 杨遵仪, 李子舜, 曲立范. 1982. 中国的三叠系. *地质学报*, (1): 1~20.
- 杨遵仪, 张舜新, 杨基端, 周惠琴, 曹洪升. 2000. 中国地层典三叠系. 北京: 地质出版社, 29~30.
- 余武, 沈传波, 杨超群. 2017. 秭归盆地中生代构造-热演化的裂变径迹约束. *地学前缘*, 24(3): 116~126.
- 张国伟, 孟庆任, 于在平, 孙勇, 周鼎武, 郭安林. 1996. 秦岭造山带的造山过程及其动力学特征. *中国科学: 地球科学*, 26(3): 193~200.
- 张国伟, 董云鹏, 赖绍聪. 2003. 秦岭-大别造山带南缘勉略构造带与勉略缝合带. *中国科学: 地球科学*, 33(12): 1121~1135.
- 张振来, 孟繁松. 1987. 长江三峡地区生物地层学(4), 三叠纪-侏罗纪分册. 北京: 地质出版社, 1~408.
- 赵金科, 陈楚震, 梁希洛. 1962. 中国的三叠系. 北京: 科学出版社, 160~191.
- 赵小明, 童金南, 姚华舟, 田洋. 2010. 三峡地区印支运动的沉积响应. *古地学报*, 12(2): 177~184.
- 周统顺, 周惠琴. 1985. 中国三叠纪陆相地层及植物群. *中国地质科学院院报*, 5: 95~111.

参 考 文 献

- 薄婧方, 姚建新, 林宝玉, 刘惟庆, 李明. 2019. 四川东部和重庆地区三叠纪海相红层分布及时代. *地质学报*, 93(2): 285~301.
- 柴嵘, 杨江海, 杜远生, 丁典岭. 2016. 鄂西秭归盆地中三叠世一早侏罗世沉积记录及其对秦岭印支碰撞造山作用的启示. *地质科技情报*, 35(4):43~49.
- 龚志愚, 张汉金, 李忠林, 罗红, 罗凡, 刘力, 杜笠超, 潘龙克. 2014. 秭归盆地沉积作用及发展演化. *资源环境与工程*, 4(28): 35~39.
- 湖北省地质矿产局. 1990. 中华人民共和国地质矿产部地质专报. 一, 区域地质. 第 20 号, 湖北省区域地质志. 北京: 地质出版社, 179.
- 湖北省地质矿产局. 1996. 全国地层多重划分对比研究——湖北省岩石地层. 武汉: 中国地质大学出版社, 187.
- 黄虎, 杨江海, 杜远生, 黄宏伟, 黄志强, 谢春霞, 胡丽沙. 2012. 右江盆地上二叠统一中三叠统凝灰岩年龄及其地质意义. *地球科学—中国地质大学学报*, 37(1): 125~138.
- 李星学, 周志炎, 蔡重阳. 1995. 中国地质时期植物群. 广州: 广东科技出版社. 229~259.
- 李旭兵, 王传尚, 刘安. 2008. 印支运动的沉积学响应——以湖北秭归盆地中, 上三叠统为例. *中国地质*, 35(5): 984~991.

Geochronological constraints on tuffs of the Badong Formation along the north margin of the Middle Yangtze region

MA Qianli^{1,2)}, CHAI Rong^{1,2)}, DU Yuansheng^{1,2)}, YANG Jianghai^{* 1,2)}, DAI Xianduo^{1,2)}

1) *State Key Laboratory of Biogeology and Environment Geology, China University of Geosciences, Wuhan, 430074;*

2) *School of Earth Sciences, China University of Geosciences, Wuhan, 430074*

** Corresponding author: yjhcug@126.com*

Abstract

The Indosinian Movement resulting in the large-scale sea-continent transition deeply changed the paleogeographical framework of the South China Continent and East Asia. The Badong Formation and related strata, which consist of carmine clastic rocks, are well developed in the north margin of the Yangtze block and represent a transition process from marine carbonate-dominated marine sedimentation to clastic rock-dominated continental deposit. The Badong Formation can be divided into three members, with member 2 marlstone sandwiched by member 1 siltstone and member 3 mudstone. Because there are few fossils found in the third member of the Badong Formation, its stratigraphic age has been controversial. This study carried out LA-ICP-MS dating for zircons from the tuff in the 2nd Member of the Badong Formation in the Zigui area. The results show that two tuff samples from the middle and top sections of the 2nd Member in the Badong Formation formed at 241.7 ± 1.7 Ma and 237.5 ± 2 Ma, respectively. The stratigraphic age of the Badong Formation, combined with emplacement age and fossil record of tuff layer, has been constrained between the Middle Triassic Anisian and the Late Triassic Carnian. Zircons in the Badong tuffs occur in elongated crystals without rounding, show obvious oscillatory zones and the similar trace elements characteristic as orogenic magmatic zircons. The top marine stratum, which is represented by the Badong Formation limestone, is distributed mainly along southeastern Hubei to western Sichuan provinces, reflecting the sea-land changing of the Upper-Middle Yangtze regions due to westward regression of seawater during the period from Middle Triassic Anisian Stage to Late Triassic Carnian Stage.

Key words: tuff; Badong Formation; Middle Yangtze; Indosinian Movement; Late Triassic